Evaluation of the Stress Pattern in the Resin-Based Composite Restoration of an Endodontically Treated Premolar Tooth: A Finite Element Analysis Study

Musliana Mustaffa[1*], Arsalan Marghoub[2], Shirin Shahrbaf[1], Nicolas Martin[1]

1. Academic Unit of Restorative Dentistry, The School of Clinical Dentistry, Claremont Crescent, Sheffield S10 2TA, UK.
2. Department of Mechanical Engineering, Faculty of Engineering Sciences, University College London, Gower Street, London WC1E 6BT, UK.

Abstract

This study aimed to assess the stress values in an endodontically treated maxillary premolar restored with a direct placement of adhesive composite restoration. An ortho-grade root-treatment was performed on a single-rooted maxillary premolar. Three types of cavities were prepared as follow: (1) O: Occlusal access cavity (one surface), (2): MO: access cavity with mesial extension equal to one third of bucco-palatal cusp width and 1 mm above the cementoenamel junction (two surfaces), (3) MOD: access cavity with mesial and distal extensions equal to one third of bucco-palatal cusp width and 1 mm above the cementoenamel junction (three surfaces). After each restorative procedure, the restored-tooth complex was scanned using a micro-computed tomography scanner. A three-dimensional (3D) structure for each individual layer, including the enamel, dentine, composite restoration, and the gutta-percha of the restored tooth complex, was generated with interactive medical image processing software, whereas the biomechanical behavior and stress pattern distribution were evaluated using a finite element analysis software programme. The results revealed that the MO-restored tooth complex showed lower stress values than the one-surface (O) and three-surface (MOD) restored cavities. The generated stress values in the two-surface (MO) restored cavity in the present study were less than that of the one-surface (O) or three-surface (MOD) restored cavities. It can be concluded that, by increasing the C-factor, higher stress values are more likely to occur in the restored tooth. Greater stress values were observed in endodontically treated tooth with MOD restoration, which might have negative consequences on the fracture strength of the whole structure.

Experimental article (J Int Dent Med Res 2022; 15(1): 53-60)
Keywords: C-factor, endodontically treated premolar, micro-CT, FEA, Von Mises stress.
Received date: 06 January 2021 **Accept date:** 03 March 2021

Introduction

Biomechanical behavior of the endodontically treated tooth restored with a direct placement of adhesive composite restoration has not been clearly investigated. Due to the methodological differences of the previous studies, such as tooth selection, type of restoration and evaluation methods, interpretation and general application are limited.

An endodontically treated tooth can be restored with a more conservative approach or an extensive restoration, depending on the amount of remaining coronal tooth structure. The best restoration should allow a restored tooth to react in a pattern similar to the sound intact tooth under occlusal loads[1] without deformation. If the remaining coronal tooth structure is adequate for a composite restoration, the material has to store an excellent quantity of energy to limit the cuspal movements,[1] and should be able to dissipate the stresses well within the structure.

Composite resin has evolved over the decades. Apart from changes in filler loading, size and shape, the monomer structure and modification of the polymerisation reaction has also been introduced.[2] This type of restorative material can be classified according to different characteristics, such as curing mechanism, viscosity and filler size. Despite having various choices of composite restorative materials,

Corresponding author:
Musliana Mustaffa
Academic Unit of Restorative Dentistry, The School of Clinical Dentistry, Claremont Crescent, Sheffield S10 2TA, UK.
E-mail: muslianamustaffa@iium.edu.my, drmusliana@gmail.com .

factors like the location of tooth to be restored, the size of cavity and aesthetic demands dictate the choice of one material over another.[2, 3]

Polymerisation shrinkage in the resin composite is a complex mechanism.[4-6] The stress can develop at the interfaces during the polymerisation process and predominantly occurs due to the contraction of the resin matrix,[5, 7-9] which compromises the dimensional stability of the restorative materials.[7] When the contraction of resin is obstructed, it is unable to resist sufficient polymerising flow to compensate for the original volume.[7] This circumstance creates rapid build-up of stress at the tooth-composite interface,[5, 10] eventually interferes with the marginal seal and potentially propagates the existing cracks.[11]

The configuration of tooth cavity, also known as the C-factor, is the ratio of the bonded to the unbonded surface.[8, 12] It has been shown to influence the formation of polymerisation shrinkage stress in the previous study[8] Other factors that may influence the formation of this stress include volumetric polymerisation shrinkage, elastic modulus, adaptation of composite resins to the internal aspect of the cavity,[8] amount of restorative material, polymerisation reaction, material's formulation[6] and cavity depth.[13]

Biomechanical behavior of the tooth under load has been measured with various methods such as photoelastic model,[14-16] strain gauge techniques,[17] two dimensional (2D) Finite Element Analysis (FEA),[18, 19] combination of strain gauges and 2D FEA,[17, 20-23] sophisticated three dimensional (3D) FEA,[24-31] and a combination of strain gauges and 3D FEA.[32] 3D FEA is now a more preferred method because it offers higher anatomic precision compared to 2D FEA,[23] morphologically more accurate resemblance of tooth[25] and more comprehensive method to evaluate the stresses developed in the entire tooth structure.[24] These advantages might explain the use of 3D FEA in other aspect in dentistry.[33]

The aim of this study is to evaluate the stress values in an endodontically treated maxillary premolar restored with a direct placement of the adhesive composite restoration.

Materials and methods

Preparation for root canal procedure

Ethical approval was obtained from the Ethical Research Committee of the School of Clinical Dentistry at the University of Sheffield, UK. An intact, single-rooted maxillary premolar tooth, with a fully formed root that was extracted for orthodontic treatment, was selected for the study.

A standard access cavity, coronal flaring with Gates Glidden drills were done on the tooth and the root canal terminus was established at 0.5 mm short of radiographic apex. Apical instrumentation was done until size 40 K Flexo files followed by a step back preparation. Cold lateral compaction was done using the ISO gutta-percha (GP) with zinc oxide eugenol-based root canal sealer. The GP was cut 2mm below the cementoenamel junction (CEJ) and vertically compacted. Glass ionomer cement (GC Fuji IX GP EXTRA GC Corporation Tokyo, Japan) (GIC) was placed 2 mm thick above the GP.

Preparation for O, MO and MOD restorations, and direct placement of the adhesive composite restoration

Occlusal restoration (one-surface restored cavity)

The restored access cavity served as an occlusal (O) restoration. The cavity was etched with 37% phosphoric acid followed by water-rinsing and air-drying. Bonding agent was applied and light cured for 10 seconds, and the cavity was restored with composite resin (Filtek^{TM} Supreme XTE Universal Restorative 3M ESPE, USA). Scanning was carried out after the completion of the occlusal restoration (O), using micro-computed tomography (micro-CT). C-factor was 5:1.

Mesio-occlusal restoration (two-surface restored cavity)

For the mesio-occlusal (MO) restoration, a cavity was prepared on the same tooth. The mesial cavity was prepared without removing the existing O restoration with the aid of an operating microscope to distinguish the tooth structure and the occlusal composite restoration. Mesial cavity dimension was prepared as follows:

Cavity width: One third of bucco-palatal cusp width

Cavity depth: 1 mm above CEJ

The restorative procedure was similar to the O restoration, and the micro-CT scanning was carried out after the completion of MO restoration. C-factor was 4:2.

Mesio-occluso-distal restoration (three-surface restored cavity)

For the mesio-occlusal-distal (MOD) restoration, a cavity was prepared on the same tooth. The distal cavity was prepared without removing the existing MO restoration with the aid of an operating microscope to distinguish the tooth structure and the O composite restoration.

Distal cavity dimension was prepared as follows:

Cavity width: One third of bucco-palatal cusp width

Cavity depth: 1 mm above CEJ

A similar technique for restoring the distal cavity was conducted, followed by micro-CT scanning. C-factor was 3:3.

Micro CT scanning

A high-resolution micro-CT scanner (Sky scan 1172 microCT; SkyScan, Aartselaar, Belgium) was used to scan the endodontically treated tooth with the O, MO and MOD restorations. A resolution of 11.65 µm (distance between slices) was selected to obtain a high-accuracy image. Reconstruction of the dataset from micro-CT scanning was done using NRecon Reconstruction software (Sky scan 1172 micro-CT; SkyScan, Aartselaar, Belgium). The reconstructed images were resized using Data Viewer software version 1.5.0.0. The output format of the acquired data was selected as a bitmap (bmp) file.

3D-image generation

Reconstruction of the 3D images was done using an interactive medical image processing software, Mimics Version 16.0 (Materialize Co. Ltd.). Voxel dimension was set similar to the slice distance, and 11.65 µm resulted in slices as thin as one voxel thick. A total number of 600 slices in each sample was involved in this process. Smoothing was done in Mimics software by using automatic smoothing function to make the STL file suitable for meshing in Hypermesh.

Finite Element Model (FEM) and load application

The images were imported to the Finite Element (FE) software (Hypermesh version 11.0, Altair Engineering Inc). This software allowed high resolution of the geometrical structure by optimising geometric editing and mesh generation, including mesh convergence test, thereby provided a direct link between geometry and FE. All structures, the dentine, enamel, GP, GIC and composite resin were assumed to be perfectly bonded to each other to allow smooth stress distribution within the structure and no defects were present at all interfaces. The types of element and number of nodes and element in all models were shown in Table 1.

Samples	Number of nodes	Number of elements	Types of element
O restoration	174, 350	916, 355	Tetrahedral
MO restoration	172, 422	905, 283	Tetrahedral
MOD restoration	170, 780	889, 738	Tetrahedral

Table 1. Number of nodes, elements and types of element in all samples.

After the 3D volume meshes, a boundary condition (zero displacement) was applied at the external root surface where all nodes were fixed in all three axes, X, Y and Z. Material properties, as shown in Table 2, were assigned to the FEM. Static vertical loading of 150 N was applied on buccal incline of palatal cusp and palatal incline of buccal cusp with a total of 300 N for all samples. The types of element and number of nodes and element in all models were shown in Table 1.

Tooth structures/ Materials	Elastic modulus/Young's modulus (MPa)	Poison ratio	References
Enamel	84, 100	0.3	13, 28, 34
Dentine	18, 600	0.31	13, 18, 26, 27, 30, 31, 35-37
Composite resin (Filtek™ Supreme XTE Universal Restorative 3M ESPE, USA)	12, 700	0.35	38
Glass Ionomer Cement (GC Fuji IX GP EXTRA GC Corporation Tokyo, Japan)	16, 900	0.3	39
Gutta percha	0.69	0.45	18, 30, 40, 41

Table 2. Material properties of tooth structures, GP and restorative materials.

Results

The cloud atlas of the von Mises stress was calculated for each sample to measure the stresses developed within each structure. The data was transformed into a color maps for a better understanding of the stresses.

The generated stress in composite resin of O restoration was higher compare to the MO and MOD restorations, possibly due to the influence of C-factor (Fig. 1).

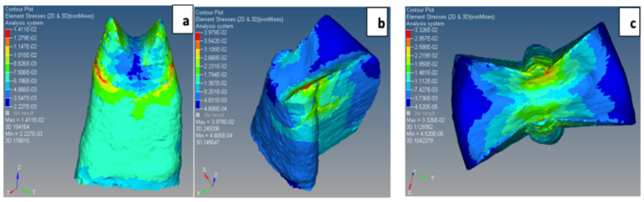

Figure 1. Distribution of stresses in composite resin of all samples. (a) O restoration; (b) MO restoration; (c) MOD restoration.

However, the generated stress in dentine of the MOD restoration was higher compared to the O and MOD restoration. This could be due to the compromised tooth structure in the MOD restoration (Fig. 2).

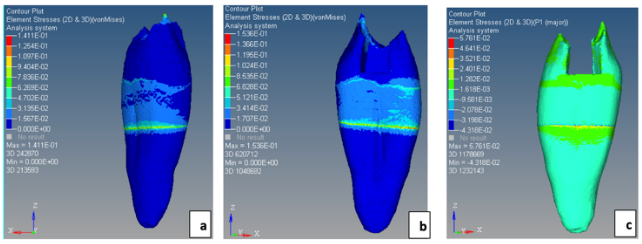

Figure 2. Distribution of stresses in dentine of all samples. (a) O restoration; (b) MO restoration; (c) MOD restoration.

With regard to the generated stress in the enamel of all types of restorations, lower stress could be seen except at the buccal and palatal regions, where the load was applied (Fig. 4). A lower generated stress pattern was also seen in the GP of all types of restorations, but the highest stress was seen at the interface of GP and GIC (Fig. 3 and 5). Based on the cloud atlas of the von Mises stress, the generated stress in GIC was higher than GP, which could be attributed to the higher elastic modulus of GIC. In addition, the generated stress at the interface of GP and GIC was higher, probably due to the huge different in the elastic modulus, interrupting the distribution of stress between these structures and resulting in the concentration of stress at the interface. Table 3 represents the peak value of von Mises stress in all structures (enamel, dentine, composite, GIC and GP) in the three types of restorations.

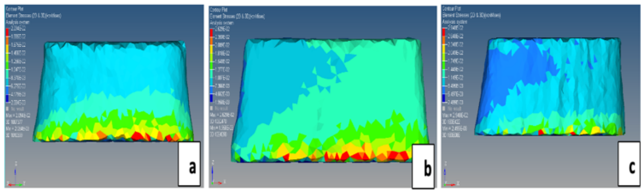

Figure 3. Distribution of stresses in GIC of all samples. (a) O restoration; (b) MO restoration; (c) MOD restoration.

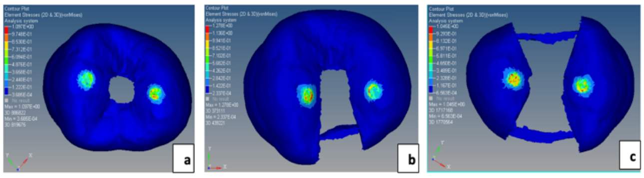

Figure 4. Distribution of stresses in enamel of all samples. (a) O restoration; (b) MO restoration; (c) MOD restoration.

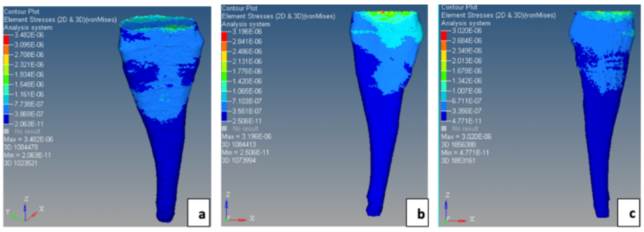

Figure 5. Distribution of stresses in GP of all samples. (a) O restoration; (b) MO restoration; (c) MOD restoration.

Samples	Enamel (MPa)	Dentine (MPa)	Composite (MPa)	GIC (MPa)	GP (MPa)
O restoration	8.54	1.11	1.28	1.68	2.35
MO restoration	1.00	1.12	3.03	2.10	2.46
MOD restoration	8.25	9.56	2.57	2.39	2.37

Table 3. Peak value of von Mises stress in all structures.

Discussion

Posterior teeth are prone to multiple forces of varying natures.[42] Therefore, the stiffness of the dental restorative materials is particularly important at the tooth-composite interfaces.[42] The software used in this study is similar to one used by,[42] and it is important to note that it is not programmed to assess model failure; it can only assess the intensity of stresses developed within the structures. The analysis of von Mises stress values revealed that lower stress values were observed in the MO restoration. This could be due to a slightly lower C-factor compared to O restoration, which made the distribution of stress in the structure appear more homogenous. Despite the MOD restoration having the lowest C-factor, the generated stress values were high, particularly in the enamel and dentine. This could be attributed to the significant loss of coronal tooth structure where the dissipation of stresses was compromised, and the generated stress was concentrated in the remaining tooth structure. Future research on mechanical testing is required to validate this data. This finding was corroborated with the other study, in which the author suggested significant stress concentration in an endodontically treated tooth with extensive restorative procedure.[26] Furthermore, greater cuspal movement was also observed in the MOD cavity preparation,[1, 43] and this might increase risk of tooth fracture. Apart from higher generated stress values in MOD restoration, higher stress concentration at the loading points in the present study was also seen, and this was corroborated with the previous studies.[1, 42]

It has been recommended to restore the tooth with the restorative materials that have an elastic modulus similar to tooth structure, so that the biomechanical behaviour of the original tooth can be to restored.[22, 44] A more specific approach is to use the restorative materials with the elastic modulus at least equal to that of a dentine[2, 45] to withstand deformation and cuspal fracture and the ability to dissipate stresses within the structure. Lower stress values and more homogenous distribution of stress were seen in the composite resins with a lower elastic modulus.[1, 42] A greater stress-dissipating effect was seen in less rigid composite compared to the more rigid restorative materials. The composite resins with low elastic modulus demonstrated a more favourable biomechanical performance.[46] Composite resins with a high elastic modulus generate higher stress in the structure,[1, 46] have less ability to absorb the stress and less able to buffer masticatory forces. Furthermore, materials with higher elastic modulus will develop higher stress values within the structure.[1] This could be due to the inability of this type of material to dissipate stresses within the structure, resulting in lack of interface harmonisation and compromised marginal integrity. Therefore, the best restoration should allow the restored tooth to react in a pattern similar to the intact tooth when the external loads are applied.[1] For this reason, the composite resin with a lower elastic modulus was used in the present study.

Of all structures involved in this study, GP had the lowest elastic modulus, almost negligible. It could be stipulated that it could be indirectly involved in transferring stresses within the whole structure. Enamel, on the other hand, showed the highest elastic modulus, and rigid enamel does not deform under stress conditions; instead, it transfers the stress to the dentine and eventually, moves over it.[24] The higher stress value observed in MOD restoration in the present study contradicted the other studies,[1, 42] possibly because the absence of a root canal procedure and the structural integrity of their model was less compromised. This might explain the differences in pattern of stress distribution even though the elastic modulus of the composite resin used in this study is almost similar.[1]

The location of the boundary condition varied greatly, including at the base of bone,[47-51] the lateral and posterior surface of bone,[52] the base and proximal surface of bone,[36] the periodontal ligament (PDL),[53, 54] the root surface[34, 42, 55] and below the CEJ,[40, 56] depending on the geometrical structures investigated. In a recent study evaluating the temporomandibular joint, the superior surface of the articular eminence was selected as a fixed boundary location.[57] Some researchers have evaluated the biomechanical behaviours of the whole unit, involving supporting tooth structures such as PDL and alveolar bone. Some researchers, on the other hand, focused only on the tooth structure under ideal circumstances where the entire facial structures could be modelled to precisely; however, this is not a pragmatic approach[58] because of the complexity of the model. Therefore, to simplify the calculations, the distance of boundary condition should be reasonable from the load application and shows no overlapping between stress and strain fields.[58] Even though the involvement of the PDL was said to be important in modelling, the accuracy of the calculated stress and strain has made biomechanical behaviour of the PDL unclear.[59] In this study, the boundary condition was set on the external root surface to address the conditions.

Static and dynamic loading are common forces used in several in vitro studies for the investigation of mechanical properties of various structures. Static loading is a constant application of load,[14, 17, 20, 60, 61] whereas dynamic loading is a repeated application of load in aqueous condition, with[62-64] or without[65, 66] thermal involvement.

Previous studies have used dynamic loading[62-67] for the evaluation of fracture strength,[62, 65] fracture mode,[63, 65, 66] survival rate,[65] microleakage,[66] the stability of implant bridgeworks [67] and also the marginal adaptation of bulk-fill composite resins.[64] To simulate this loading, either a computer-controlled chewing simulator[62, 67] or a cyclic loading machine[65, 66] was used to create a chewing condition for fatigue testing. This could theoretically represent the chewing mechanism in the mouth; the human masticatory system is a dynamic process involving forces generated by the active muscles for determination of jaw movement and joint loading,[68] To date, there is still no investigation of the dynamic loading in FEA, because the simulation of dynamic modelling requires masticatory muscles and temporomandibular joint involvement, which is difficult to standardise. Such complexity could complicate the present study;[68] therefore, a static loading was used in this study because it was more appropriate to evaluate biomechanical behaviour of the structure.

The magnitude of the load in the previous studies ranged from 1 N[18, 19] to 400 N[15, 24] to simulate the mastication load. Higher load is rarely applied for biomechanical analysis because there is no resemblance to a clinical situation. It was predicted in a previous study [24] that the load between 700 N and 800 N can cause tooth fractures. Static loading was used in several studies by applying load vertically,[14, 18, 24, 26, 27] oblique at 30 degrees,[14] 45 degree,[15, 16, 26, 29] 135 degrees[19] and perpendicular[22] to the long axis of the tooth, depending on the sample or tooth type. Due to the wide range of load magnitude, the average masticatory load of a premolar tooth, 300 N[31] was applied to the model due to its clinical relevance.

Conclusions

Within the limitation of the present study, the conclusions were:

1. Lower stress values were seen in MO restoration.
2. By increasing the C-factor, it is more likely to have higher stress values in the restored tooth.
3. Greater stress values were observed in an endodontically treated tooth with MOD restoration, which might have negative consequences on the fracture strength of the whole structure.

Acknowledgements

This research did not receive any research grant from the public or private sectors.

Declaration of Interest

The authors report no conflict of interest.

References

1. Ausiello P, Apicella A, Davidson CL, Rengo S. 3D-finite element analyses of cusp movements in a human upper premolar, restored with adhesive resin-based composites. J Biomech 2001;34(10):1269-1277.
2. Ilie N, Hickel R. Resin composite restorative materials. Aust Dent J 2011;56:59-66.
3. Hervás-García A, Martínez-Lozano MA, Cabanes-Vila J, Barjau-Escribano A, Fos-Galve P. Composite resins. A review of the materials and clinical indications. Med Oral Patol Oral Cir Bucal 2006;11(2):E215-220.
4. Terry D, Leinfelder K. Composite resin restorations: a simplified approach. ActaBiomaterialia 2. 2006:633,639.
5. Antonucci JM, Giuseppetti AA, O'Donnell JN, Schumacher GE, Skrtic D. Polymerization stress development in dental composites: Effect of cavity design factor. Materials. 2009;2(1):169-180.
6. Schneider LFJ, Cavalcante LM, Silikas N. Shrinkage Stresses Generated during Resin-Composite Applications: A Review. J Dent Biomech. 2010.
7. Davidson CL, Feilzer AJ. Polymerization shrinkage and polymerization shrinkage stress in polymer-based restoratives. J Dent 1997;25(6):435-440.
8. Ghulman MA. Effect of cavity configuration (C factor) on the marginal adaptation of low-shrinking composite: a comparative ex vivo study. Int J Dent 2011.
9. Lopes MB, Serralvo AD, Felizardo KR, et al. Evaluation of the flexural resistance and stress contraction of a silorane-based composite submitted to different protocols of polymerization. Applied Adhesion Science 2014;2(23):1-8.
10. Pereira RA, Araujo PA, Castaneda-Espinosa JC, Mondelli RF. Comparative analysis of the shrinkage stress of composite resins. J Appl Oral Sci 2008;16(1):30-34.
11. Tantbirojn D, Versluis A, Pintado MR, DeLong R, Douglas WH. Tooth deformation patterns in molars after composite restoration. Dent Mater 2004;20(6):535-542.
12. Ishikiriama SK, Valeretto TM, Franco EB, Mondelli RFL. The influence of "C-factor" and light activation technique on polymerization contraction forces of resin composite. J Appl Oral Sci 2012;20(6):603-606.
13. Chuang SF, Chang CH, Chen TY. Contraction behaviors of dental composite restorations--finite element investigation with DIC validation. J Mech Behav Biomed Mater 2011;4(8):2138-2149.
14. Assif D, Oren E, Marshak BL, Aviv I. Photoelastic analysis of stress transfer by endodontically treated teeth to the supporting structure using different restorative techniques. J Prosthet Dent

1989;61(5):535-543.
15. Yamamoto M, Miura H, Okada D, Komada W, Masuoka D. Photoelastic stress analysis of different post and core restoration methods. Dent Mater J 2009;28(2):204-211.
16. Ma J, Miura H, Okada D, Yusa K. Photoelastic stress analysis of endodontically treated teeth restored with different post systems: normal and alveolar bone resorption cases. Dent Mater J 2011;30(6):806-813.
17. Morin DL, Douglas WH, Cross M, DeLong R. Biophysical stress analysis of restored teeth: experimental strain measurement. Dent Mater 1988;4(1):41-48.
18. Ko CC, Chu CS, Chung KH, Lee MC. Effects of posts on dentin stress distribution in pulpless teeth. J Prosthet Dent 1992;68(3):421-427.
19. Soares CJ, Castro CG, Santos Filho PC, Soares PV, Magalhaes D, Martins LR. Two-dimensional FEA of dowels of different compositions and external surface configurations. J Prosthodont 2009;18(1):36-42.
20. Morin DL, Cross M, Voller VR, Douglas WH, DeLong R. Biophysical stress analysis of restored teeth: modelling and analysis. Dent Mater 1988;4(2):77-84.
21. Reeh ES, Ross GK. Tooth stiffness with composite veneers: a strain gauge and finite element evaluation. Dent Mater 1994;10(4):247-252.
22. Magne P, Versluis A, Douglas WH. Rationalization of incisor shape: experimental-numerical analysis. J Prosthet Dent. 1999;81(3):345-355.
23. Soares PV, Santos-Filho PC, Martins LR, Soares CJ. Influence of restorative technique on the biomechanical behavior of endodontically treated maxillary premolars. Part I: fracture resistance and fracture mode. J Prosthet Dent 2008;99(1):30-37.
24. Ausiello P, Apicella A, Davidson CL. Effect of adhesive layer properties on stress distribution in composite restorations--a 3D finite element analysis. Dent Mater 2002;18(4):295-303.
25. Boschian Pest L, Guidotti S, Pietrabissa R, Gagliani M. Stress distribution in a post-restored tooth using the three-dimensional finite element method. J Oral Rehabil 2006;33(9):690-697.
26. Jiang W, Bo H, Yongchun G, LongXing N. Stress distribution in molars restored with inlays or onlays with or without endodontic treatment: a three-dimensional finite element analysis. J Prosthet Dent 2010;103(1):6-12.
27. Eraslan Ö, Eraslan O, Eskitaşcıoğlu G, Belli S. Conservative restoration of severely damaged endodontically treated premolar teeth: a FEM study. Clin Oral Investig 2011;15(3):403-408.
28. Kantardžić I, Vasiljević D, Blažić L, Lužanin O. Influence of cavity design preparation on stress values in maxillary premolar: a finite element analysis. Croat Med J 2012;53(6):568-576.
29. Watanabe MU, Anchieta RB, Rocha EP, et al. Influence of crown ferrule heights and dowel material selection on the mechanical behavior of root-filled teeth: a finite element analysis. J Prosthodont 2012;21(4):304-311.
30. Rippe MP, Santini MF, Bier CA, Borges AL, Valandro LF. Root canal filling: fracture strength of fiber-reinforced composite-restored roots and finite element analysis. Braz Dent J 2013;24(6):619-625.
31. Shahrbaf S, vanNoort R, Mirzakouchaki B, Ghassemieh E, Martin N. Effect of the crown design and interface lute parameters on the stress-state of a machined crown-tooth system: a finite element analysis. Dent Mater 2013;29(8):e123-e131.
32. Tajima K, Chen KK, Takahashi N, Noda N, Nagamatsu Y, Kakigawa H. Three-dimensional finite element modeling from CT images of tooth and its validation. Dent Mater J 2009;28(2):219-226.
33. Augustine C, Soegiharto BM. Stress distribution of anterior tooth apex and their surrounding alveolar bone during maxillary anterior intrusion on segmented and continuous wires (3D Finite Element Analysis). J Int Dent Med Res 2018; 11(2): 596-601.
34. Sorrentino R, Aversa R, Ferro V, et al. Three-dimensional finite element analysis of strain and stress distributions in endodontically treated maxillary central incisors restored with different post, core and crown materials. Dent Mater 2007;23(8):983-993.
35. Coelho CS, Biffi JC, Silva GR, Abrahao A, Campos RE, Soares CJ. Finite element analysis of weakened roots restored with composite resin and posts. Dent Mater J 2009;28(6):671-678.
36. Dejak B, Młotkowski A. 3D-Finite element analysis of molars restored with endocrowns and posts during masticatory simulation. Dent Mater 2013;29(12):e309-e317.
37. Durand LB, Guimarães JC, Monteiro Junior S, Baratieri LN. Effect of ceramic thickness and composite bases on stress distribution of inlays--a finite element analysis. Braz Dent J 2015;26(2):146-151.
38. Yamanel K, Caglar A, Gülsahi K, Ozden UA. Effects of different ceramic and composite materials on stress distribution in inlay and onlay cavities: 3-D finite element analysis. Dent Mater J 2009;28(6):661-670.
39. Romeed SA, Dunne SM. Stress analysis of different post-luting systems: a three-dimensional finite element analysis. Aust Dent J 2013;58(1):82-88.
40. Liu HL, Lin CL, Sun MT, Chang YH. Numerical investigation of macro- and micro-mechanics of a ceramic veneer bonded with various cement thicknesses using the typical and submodeling finite element approaches. J Dent 2009;37(2):141-148.
41. Adıgüzel Ö, Kaya S, Yigit - Ozer S, Değer Y, Göncü Başaran E, Yavuz I. Three-dimensional Finite Element Analysis of Endodontically Treated Tooth Restored with Carbon and Titanium Posts. International Dental Research 2011;1(2):55-59.
42. Ausiello P, Rengo S, Davidson CL, Watts DC. Stress distributions in adhesively cemented ceramic and resin-composite Class II inlay restorations: a 3D-FEA study. Dent Mater 2004;20(9):862-872.
43. Jantarat J, Panitvisai P, Palamara JE, Messer HH. Comparison of methods for measuring cuspal deformation in teeth. J Dent 2001;29(1):75-82.
44. Bojar W, Walke W. FEM Analysis of Lower Premolar Root Canal Filling. Solid State Phenomena 2012;183:17-24.
45. El-Safty S, Akhtar R, Silikas N, Watts DC. Nanomechanical properties of dental resin-composites. Dent Mater 2012;28(12):1292-1300.
46. Lin CL, Chang YH, Liu PR. Multi-factorial analysis of a cusp-replacing adhesive premolar restoration: A finite element study. J Dent 2008;36(3):194-203.
47. Magne P. Virtual prototyping of adhesively restored, endodontically treated molars. J Prosthet Dent 2010;103(6):343-351.
48. Benazzi S, Kullmer O, Grosse IR, Weber GW. Using occlusal wear information and finite element analysis to investigate stress distributions in human molars. J Anat 2011;219(3):259-272.
49. Moga RA, Chiorean CG. Strain Analysis of a Human Tooth with Support Tissues Resorption. In Proceedings of the World Congress on Engineering 2013;Vol 2.
50. Kainose K, Nakajima M, Foxton R, Wakabayashi N, Tagami J. Stress distribution in root filled teeth restored with various post and core techniques: effect of post length and crown height. Int Endod J 2015;48(11):1023-1032.
51. Singh SV, Bhat M, Gupta S, Sharma D, Satija H, Sharma S. Stress distribution of endodontically treated teeth with titanium alloy post and carbon fiber post with different alveolar bone height: A three-dimensional finite element analysis. Eur J Dent 2015;9(3):428-432.
52. Croci CS, Caria PHF. Rotation axis of the maxillary molar and maximum tooth movement according to force direction. Braz J Oral Sci 2015;14(2):130-134.
53. Gomes ÉA, Gueleri DB, da Silva SR, Ribeiro RF, Silva-Sousa YT. Three-dimensional finite element analysis of endodontically treated teeth with weakened radicular walls restored with different protocols. J Prosthet Dent 2015;114(3):383-389.
54. Zelic K, Vukicevic A, Jovicic G, Aleksandrovic S, Filipovic N, Djuric M. Mechanical weakening of devitalized teeth: three-dimensional Finite Element Analysis and prediction of tooth fracture. Int Endod J 2015;48(9):850-863.
55. Ausiello P, Franciosa P, Martorelli M, Watts DC. Numerical fatigue 3D-FE modeling of indirect composite-restored posterior teeth. Dent Mater 2011;27(5):423-430.
56. Huang Z, Chen Z. Three-dimensional finite element modeling of a maxillary premolar tooth based on the micro-CT

scanning: a detailed description. J Huazhong Univ Sci Technolog Med Sci 2013;33(5):775-779.
57. Su YH, Hsu ML. Biomechanical evaluation of temporomandibular joint disc by using 3-D Finite Element Analysis during loading. J Int Dent Med Res 2019;12(2): 377-382.
58. Moeen F, Nisar S, Dar N. A step by step guide to finite element analysis in dental implantology. Pakistan Oral & Dental Journal 2014;34(1):161-169.
59. Chang CH, Lei YN, Ho YH, Sung YH, Lin TS. Predicting the holistic force-displacement relation of the periodontal ligament: in-vitro experiments and finite element analysis. Biomed Eng Online 2014;13(1):1-11.
60. Sakaguchi RL, Brust EW, Cross M, DeLong R, Douglas WH. Independent movement of cusps during occlusal loading. Dent Mater 1991;7(3):186-190.
61. Plotino G, Buono L, Grande NM, Lamorgese V, Somma F. Fracture resistance of endodontically treated molars restored with extensive composite resin restorations. J Prosthet Dent 2008;99(3):225-232.
62. Heydecke G, Butz F, Hussein A, Strub JR. Fracture strength after dynamic loading of endodontically treated teeth restored with different post-and-core systems. J Prosthet Dent 2002;87(4):438-445.
63. Sterzenbach G, Rosentritt M, Frankenberger R, Paris S, Naumann M. Loading standardization of postendodontic restorations in vitro: impact of restorative stage, static loading, and dynamic loading. Oper Dent 2012;37(1):71-79.
64. Campos EA, Ardu S, Lefever D, Jassé FF, Bortolotto T, Krejci I. Marginal adaptation of class II cavities restored with bulk-fill composites. J Dent 2014;42(5):575-581.
65. Xible AA, Tavarez RRDJ, Araujo CDRPD, Conti PCR, Bonachella WC. Effect of cyclic loading on fracture strength of endodontically treated teeth restored with conventional and esthetic posts. J Appl Oral Sci 2006;14(4):297-303.
66. Jung SH, Min KS, Chang HS, Park SD, Kwon SN, Bae JM. Microleakage and fracture patterns of teeth restored with different posts under dynamic loading. J Prosthet Dent 2007;98(4):270-276.
67. Karl M, Fischer H, Graef F, Wichmann MG, Taylor TD, Heckmann SM. Structural changes in ceramic veneered three-unit implant-supported restorations as a consequence of static and dynamic loading. Dent Mater 2008;24(4):464-470.
68. Koolstra JH. Dynamics of the human masticatory system. Crit Rev Oral Biol Med 2002;13(4):366-376.